HHS Public Access

Author manuscript

Bone Marrow Transplant. Author manuscript; available in PMC 2019 April 03.

Published in final edited form as:

Bone Marrow Transplant. 2019 July ; 54(7): 973–979. doi:10.1038/s41409-018-0352-9.

Pre-transplant expressions of microRNAs, comorbidities, and post-transplant mortality

Mohamed L. Sorror, MD, MSc[1,2], **Ted A. Gooley, PhD**[1,2], **Kirsteen H. Maclean, PhD**[3], **Jesse Hubbard, B.S**[1], **Mario A. Marcondes, MD, PhD**[1,2], **Beverly J. Torok-Storb, PhD**[1,2], and **Muneesh Tewari, MD, PhD**[4]

[1]Fred Hutchinson Cancer Research Center

[2]University of Washington

[3]NanoString Technologies, Seattle, WA

[4]University of Michigan, Ann Arbor, MI.

Abstract

We analyzed micro-RNAs (miRs) as possible diagnostic biomarkers for relevant comorbidities prior to and prognostic biomarkers for mortality following hematopoietic cell transplantation (HCT). A randomly selected group of patients (n=36) were divided into low-risk (HCT-comorbidity index [HCT-CI] score of 0 and survived HCT) and high-risk (HCT-CI scores ≥4 and deceased after HCT) groups. There were 654 miRs tested and 19 met the pre-specified significance level of $p<0.1$. In subsequent models, only eight miRs maintained statistical significance in regression models after adjusting for baseline demographic factors; miRs-374b and −454 were under-expressed, while miRs-142–3p, −191, −424, −590–3p, −29c, and −15b were over-expressed among high-risk patients relative to low-risk patients. Areas under the curve for these 8 miRs ranged between 0.74 to 0.81, suggesting strong predictive capacity. Consideration of miRs may improve risk-assessment of mortality and should be further explored in larger future prospective studies.

Keywords

allogeneic transplants; comorbidities; micro-RNA; mortality; risk-assessment

Correspondence to: Mohamed L. Sorror, M.D., Clinical Research Division (D5-280), Fred Hutchinson Cancer Research Center, 1100 Fairview Avenue North, Seattle, WA 98109-1024, Telephone: 206-667-6298, Fax 206-667-5899, msorror@fredhutch.org.

Author contributions: MLS, BTS, and MT contributed to study design; MLS collected data and obtained funding for the study; MLS and JH contributed to sample analyses; TG performed statistical analysis; MLS, KM, JH, MAM, BTS, and MT contributed to analysis and interpretation of results; MLS wrote the manuscript; MLS, MAM, BTS, and MT edited the manuscript.

Conflict of interest: Dr. Maclean is employed by NanoString Technologies, which provided the assay to determine expressions of miRs. Dr. Sorror, Dr. Gooley, Mr. Hubbard, Dr. Marcondes, Dr. Torok-Storb, and Dr. Tewari declare no potential conflict of interest.

Conflict of interest statement: Kirsteen H. Maclean is employed by NanoString Technologies, which provided the assay to determine expressions of miRs; otherwise, the authors have no competing interests.

INTRODUCTION

Allogeneic hematopoietic cell transplantation (HCT) is a potentially curative treatment for many patients with hematological diseases. Success of HCT relies greatly on accurate pre-transplant risk-assessment. The HCT-comorbidity index (CI) was developed as a measure of health-status that could quantify the magnitude of organ dysfunctions before and could stratify mortality risk following HCT (1). Further, information is required to determine the underlying association between biologic tissue-specific processes related to comorbidities and post-transplant mortality. Such biological processes could serve as novel biomarkers that could improve pre-HCT comorbidity screening and improve the prognostic power for post-HCT mortality.

Here, we analyzed in a preliminary study plasma micro-RNAs (miRs) as a novel and potentially powerful biomarker approach for prediction of HCT outcomes. MiRs are a class of small non-coding RNAs (~22 nt) that negatively regulate gene expression by pairing with partially complementary target sequences in the 3' untranslated regions of messenger RNAs (mRNAs) to block translation and/or promote mRNA degradation (2). They control activity of ~30% of all protein-coding genes with an average of ~200 mRNA targets per miR molecule (3). A series of studies has uncovered the functional role of miRs in diverse biological and pathophysiological processes including cardiac, vascular, hepatic (4), and autoimmune diseases (5).

Recent discoveries suggested a strong role of miR-423, miR-199a-3p, miR-93*, and miR-377, miR-146a, and miR-155 in predicting probability of acute graft versus-host disease (GVHD) (6–9). However, these miRs were evaluated after HCT, which limits the ability to use them in pre-transplant decision making. To date, no dedicated analysis of associations between pre-transplant miRs and mortality has been done. To this end, we took an initial step in this process, as a proof of concept, by examining associations between pre-transplant miRs, comorbidities, and post-transplant mortality.

SUBJECTS AND METHODS

Subjects

Informed consent was collected from patients at the time of donation of their blood sample for research purposes. Because this is a retrospective study, no new consent form was collected. The study was approved by the Fred Hutchinson Cancer Research Center Internal Review Board (IRB).

Study participants had the following criteria 1) diagnosis of acute myeloid (AML) or lymphoid (ALL) leukemia, 2) were in complete remission before HCT, 3) received HLA-matched peripheral blood mononuclear cell (PBMC) grafts, 4) had PBMC previously collected and stored within 30 days prior to HCT, and 5) treated with allogeneic HCT between 2005 and 2009. Of the 140 patients that met these criteria, 36 were randomly selected that met one of two other criteria: had pre-transplant HCT-CI scores of 0 and survived HCT per last-follow up (low-risk, n=18) or had HCT-CI scores of ≥4 and died after HCT (high-risk, n=18). Comorbidities were scored per the HCT-CI (1, 10). We collected

information on causes of death (COD) as stratified into: root COD defined as the underlying cause, contributing COD defined as other ongoing problems leading to and contributing to death, and proximate COD defined as the most significant recent cause to deterioration of patient health before death.

MiR Analysis

All samples were collected in ethylenediaminetetraacetic (EDTA) acid tubes and processed and frozen at −80 ºC within 8 hours of draw. RNA was isolated from PBMC per previous methods (11). For discovery of potentially relevant miRs, we used the NanoString nCounter miR assay as previously described (12). Analysis of miR raw data was done using nSolverTM 2.0 Software (NanoString Technologies, Inc.) applying standard quality control tests.

Overview of Nanostring Methodology

To develop and optimize a clinically relevant method for the identification of novel biomarkers for relevant comorbidities before and prognostic biomarkers for mortality after HCT, we utilized an assay based on the recently described NanoString multiplex platform (nCounter) incorporating fluorescent barcodes together with a digital readout for single-molecule imaging (13). In contrast to other miR profiling technologies, the NanoString platform does not involve reverse transcription; instead the technology relies on sequence-specific probes to digitally measure the copy number (DNA), target (i.e., mRNA), or small RNA (e.g. mature miR) abundance. Through the use of a chimeric mature miR-miRTag sequence, the nCounter miR assays can therefore accurately distinguish between highly homologous miR family members with great specificity, without the need for enzymatic amplification (14). The NanoString miR pre-designed panel simultaneously detects 673 human miRs including five housekeeping transcripts [(actin beta (NM_001101.2), beta-2 microglobulin (NM_004048.2), GAPDH (NM_002046.3), RPL19 (NM_000981.3), and RPLP0 (NM_001002.3)], six positive, and eight negative controls (proprietary spike-in controls to determine sample integrity as well as efficiency and background).

Each human miR of interest is detected using a specific pair of probes called the reporter and capture probes. Each probe within a probe pair contains miR-specific sequences that together recognize a 100-base contiguous region within the targeted miR. In addition, the reporter probes carry a color code at the 5’ end that enables the molecular barcoding of the miRs of interest, while the capture probes carry a biotin label at the 3’ end that provides a molecular handle for the attachment of target genes to facilitate downstream digital detection. The color code on each reporter probe has six positions, each of which can be one of four spectrally non-overlapping fluorescent colors. The different combinations of the four distinct colors at six contiguous positions allows for a large diversity of color-based barcodes, each designating a different mature miR sequence that can be mixed together in a single reaction for hybridization and still be individually resolved and identified. This allows a large diversity of targets present in the same sample to be individually resolved and identified during data collection. It is theoretically possible to generate 46 different color codes, each barcoding a distinct small RNA. However, the kinetics of solution-phase

hybridization and the technology for digital detection of different color barcodes currently limit the measurement power to less than a thousand miR species.

Methodology

RNA extraction.—The use of control RNA included in the nCounter Human miR Sample Preparation Kit allows the user to monitor the ligation efficiency and specificity through each step of the reaction, thereby serving as a control for integrity and quality of the total RNA as well as the purified miR samples. Recovery of these 6 different synthetic miRs also provides confidence that that the Nanostring nCounter system performs as expected.

miR expression profiling.—The digital multiplexed NanoString nCounter human miR expression assay (NanoString Technologies) was performed with 100 ng total RNA as input material according to the NanoString miR Assay Manual. Small RNA samples were prepared by ligating a specific DNA tag (miR-tag) onto the 3' end of each mature miR according to the manufacturer's instructions (NanoString Technologies). These tags serve several purposes: 1) to normalize the wide range of melting temperatures (Tms) of the miRs; 2) to provide a template to facilitate the use the NanoString dual probe system; 3) to enable single base pair discrimination and specificity of highly homologous miR family members; and 4) to provide identification for each miR species in the sample. Excess tags were then removed with the use of a restriction digest at 37^{o}C. The resulting material was incorporated into an overnight hybridization reaction. Hybridizations were carried out by combining 5 μl of each miR-miRTag sample with 20 μl of nCounter Reporter probes in hybridization buffer and 5 μl of nCounter Capture probes for a total reaction volume of 30 μl. The hybridizations were incubated at 65°C for approximately 16 to 20 hours. During the overnight hybridization reaction, probe pairs are present in large excess to target small RNAs to ensure that each target finds a probe pair.

Overview of thermocycling conditions.—The nCounter miR Preparation protocol requires careful temperature control of all reaction steps. A thermocycler with a heated lid is critical for this procedure.

Annealing Protocol: Temperature Time

94°C 1 min

65°C 2 min

45°C 10 min

48°C hold

Total Time 13 min

Ligation Protocol: Temperature Time

48°C 3 min

47°C 3 min

46°C 3 min

45°C 5 min

65°C 10 min

4°C hold

Total Time 24 min

Purification Protocol: Temperature Time

37°C 2 hours

70°C 10 min

4°C hold

Total Time 2 hours 10 min

nCounter Prep station.—The nCounter Prep Station is the automated fluidic handling component of the nCounter System and processes samples post-hybridization to prepare them for data collection on the nCounter Digital Analyzer. Excess probes are washed away using a two-step magnetic bead based purification on the nCounter Prep Station. Magnetic beads derivatized with short nucleic acid sequences that are complementary to the Capture Probe and the Reporter Probes are used. First, the hybridization mixture containing target/probe complexes is allowed to bind to magnetic beads complementary to sequences on the Capture Probe and washed followed by a sequential binding to sequences on the Reporter Probe. Biotinylated capture probe-bound miR-miRtags are immobilized and recovered on a streptavidin-coated cartridge using the nCounter PrepStation (nanoString Technologies). Abundances of specific miR molecules can then be quantified using the nCounter Digital Analyzer to count the individual fluorescent barcodes and assess target miR molecules present in each sample. For each assay, a high-density scan (encompassing 600 fields of view) was performed.

nCounter Digital Analyzer.—The nCounter Digital Analyzer collects data by taking images of the immobilized fluorescent reporters in the sample cartridge with a CCD camera through a microscope objective lens. At the highest standard data resolution, 600 fields of view (FOV) are collected per flow cell (sample), yielding data of hundreds of thousands of target molecule counts. The number of images taken corresponds to the number of reporters counted and this, in part, determines the dynamic range and level of sensitivity in the system. Images are processed internally, and the results are exported as a comma-separated values format file that can be downloaded via memory stick. The file can be opened by most commonly used spreadsheet packages, including Microsoft® Excel, exported to other data visualization packages, or normalized using the NanoString nSolver software analysis tool.

Data Analysis and Statistical Methods

All data analysis was performed using the nSolver software analysis (freely available for download from NanoString Technologies). A comprehensive manual outlining all strategies for data analysis and normalization of miR data accompanies the use of the software tool. Heat maps were created to show median-centered expression of each gene using Cluster 3.0 and JavaTreeView software algorithms applied to log2 transformed data.

All samples contributed to the discovery analysis. MiRs were filtered to include only those expressed with at least 50 counts for the NanoString abundance analyses. MiR raw data was normalized using the geometric mean of top 100 miRs (probes with highest 100 counts) as recommended by the manufacturer. Fold-change was calculated with partitioning by the low- versus high-risk groups computing a two-tailed t-test on the log-transformed normalized data that assumes unequal variance. We used a p-value cut-off of <0.1 to identify potentially relevant miRs. Heat-map analysis used z-score transformation on samples computing Spearman correlation of the medians between two samples of 8 patients from each group.

We then compared the mean expression level between low- and high-risk patients for each of the 19 miRs identified from the initial examination using linear regression with adjustment for diagnosis, conditioning intensity, donor type, age (continuous variable), gender, and race. All p-values from regression models are two-sided.

We also fit multivariable logistic regression models (with the same adjustments as listed above) for the outcome high risk vs. low risk with miR expression as an exploratory variable. This effectively is the same model as the linear regression models above with miR expression as the outcome, but the logistic regression models allow one to estimate the area under the curve (AUC) associated with each miR in terms of separation of expression level between the two risk groups. An optimal expression cutoff for each miR was then estimated by maximizing Youden's J index (which corresponds to the threshold leading to the point on the receiver operating characteristic (ROC) curve that maximizes the vertical distance between the ROC curve and the non-informative diagonal line), and the associated odds ratio for expression levels above the appropriate threshold vs. expression levels below the threshold was estimated for the outcome defining risk (low risk vs. high risk).

With 18 patients in each of the risk groups, we have 85% power to observe a statistically significant difference (at the two-sided significance level of .05) in mean expression levels if the true distributions are separated by one standard-deviation unit.

Finally, even though the study was designed to look only at associations between miRs and mortality, we examined whether any of detected miRs is associated with development of grades II-IV or III-IV acute GVHD. This was done using multivariate regression models treating miRs as continuous variables.

RESULTS

Patient Characteristics

Overall patient characteristics are summarized in Table 1. HLA-matched unrelated grafts were given to 83% and 72% of the low- and high-risk groups, respectively, while remaining patients received HLA-identical-sibling grafts. Diagnoses were AML in 78% and 67%, respectively, while remaining diagnoses were ALL. The majority of patients were in first CR (67% and 61%, respectively), while remaining patients were in second CR. Finally, 50% and 39% of patients, respectively, received high-dose conditioning regimens, while remaining patients received reduced-intensity regimens.

Cause of Death

There were multiple COD for the 18 high-risk patients with increased expressions of the 8 miRs. Six patients (33.3%) had multiple organ failure with or without infections and acute GVHD. Five patients (27.8%) died from acute GVHD alone or coupled with cardiac complications such as heart failure. Four other patients (22.2%) died from infections alone or with heart or respiratory failures. Two patients died from cerebro-vascular strokes. One patient died from idiopathic pneumonia syndrome and respiratory failure.

Analysis of miRs expression among high vs. low risk groups

Among 654 tested miRs, 19 met the pre-specified significance level of $p<0.1$. Among those 19 miRs, 7 were under-expressed, while 12 miRs were over-expressed before HCT among high- versus low-risk groups, respectively (Table 2 and Figure 1). In linear regression models for each of these 19 miRs, only 8 maintained statistically significant ($p \leq .05$) differences between the two risk groups after adjustment for the factors defined under “Methods” above. Of the eight miRs, 2 were under-expressed [miR-374b ($p = 0.03$), miR-454 ($p = 0.04$)] and 6 were over-expressed [miR-142–3p ($p=.05$), miR-191 (p = 0.02), miR-424 (p = 0.04), miR-590–3p (p = 0.03), miR-29c (p=.03), and miR-15b (p = 0.05)] among high- versus low-risk groups as summarized in Table 3.

AUC results for these 8 miRs ranged between 0.74 to 0.81 (Table 3). Odds ratios for low-risk assignment when comparing patients with low (below the “optimal” threshold as defined above) vs. high (above the optimal threshold) expression ranged between 0 (eight of 8 low-expression patients were in low-risk category compared to 10 of 28 high-expression patients) and infinity (seven of 7 high-expression patients were in low-risk category compared to 11 of 29 low-expression patients).

In separate multivariate models where the 8 miRs were modeled as continuous variables, we found miR-15b (Odds ratio: 1.0005, p=0.03) and miR-191 (Odds ratio: 1.002, p=0.04) to be associated with development of grades III-IV acute GVHD.

DISCUSSION

We identified a group of 8 miR biomarkers as potentially being associated with post-transplant mortality risk. Each of these 8 miRs were previously shown to predict the burden of some comorbidities including cardiac, pulmonary, hepatic, renal, autoimmune and

rheumatologic comorbidities, as well as psychiatric disease, inflammatory bowel disease, obesity, infection, diabetes, central nervous system disease, and malignancies (for example (15–34)). While a number miRs were previously shown to predict development of acute GVHD, those miRs were tested after onset of HCT, limiting their use in decision-making before HCT (6–8). Here, we used miRs as novel molecular biomarkers of mortality risks but evaluated them before the onset of conditioning regimens. Our results suggest that patients with significant comorbidities might have abnormal expressions of miRs that could be detected before HCT, hence providing a more objective evaluation of comorbidities. We hypothesize that the abnormally expressed miRs set the stage for the development of post-HCT morbidities such as GVHD, infection, and organ failures, as demonstrated in COD, regardless of baseline variables such as characteristics of primary cancer or transplant type.

MiRs are remarkably stable. Tissue-derived miRs can easily reach the circulation where they are readily detectable in a cell-free form, potentially providing a route for minimally invasive detection (35). Recent data suggest that miRs are actively secreted from cells in 50–90 nm membrane-bound particles called exosomes, which may account for their stability in the bloodstream (36). This active secretion mechanism may enable the accumulation of miRs in plasma to relatively high levels as compared to other nucleic acid markers (e.g., DNA) that are released only upon cell lysis.

No adjustments were made for multiple comparisons, either in the discovery phase or in the linear regression models, because at this exploratory stage of examination of the studied miRs we were more concerned with type-II errors than type-I errors. Therefore, results should be confirmed in a larger study. Moreover, we showed only that these miRs had differential expression among low- vs. high-risk groups, and these groups were defined based on having an HCT-CI of 0 and surviving (low-risk group) or having an HCT-CI of 4 or more and dying (high-risk group). In this sense, these groups were chosen to be at the extremes, so that if an association between miR and outcome exists, looking at the extreme groups would provide the best chance of identifying a potential signal. The current results, therefore, provide a list of miRs that are merely candidates and that deserve further exploration in a study that does not restrict the population based on HCT-CI and/or outcome.

The previous limitations not withstanding, our results are novel and have significant clinical and scientific applications. Development of a MiR-based measure of health status in a new prospective study could improve our ability of accurate detection of relevant organ dysfunctions prior to HCT and early prediction of HCT-related morbidity and mortality. Information could be used to better determine patient eligibility for transplants and for different conditioning intensity, to assign patients to trials investigating interventions that could alleviate the burden of pre-HCT organ dysfunctions, and to decrease the risk of a given HCT-related complication.

ACKNOWLEDGEMENTS

Sources of funding. This study was supported by grants DK056465, HL099993, and HL088021 from the National Institutes of Health. M.L.S. is also supported by a Research Scholar Grant No. RSG-13-084-01-CPHPS from the American Cancer Society (ACS) and a Contract No. CE-1304-7451 from the Patient-Centered Outcome Research Institute (PCORI).

We are grateful to Gary Schoch for acquisition of data. We would like to thank Bonnie Larson, Helen Crawford, and Jennifer E. Nyland for their assistance with manuscript preparation.

Sources of funding. This study was supported by grants DK056465, HL099993, and HL088021 from the National Institutes of Health. M.L.S. is also supported by a Research Scholar Grant No. RSG-13-084-01-CPHPS from the American Cancer Society (ACS) and Contract No. CE-1304-7451 from the Patient-Centered Outcome Research Institute (PCORI).

REFERENCES

1. Sorror ML, Maris MB, Storb R, Baron F, Sandmaier BM, Maloney DG, et al. Hematopoietic cell transplantation (HCT)-specific comorbidity index: a new tool for risk assessment before allogeneic HCT. Blood 2005;106(8):2912–9. [PubMed: 15994282]
2. Lu M, Zhang Q, Deng M, Miao J, Guo Y, Gao W, et al. An analysis of human microRNA and disease associations. PLoS ONE 2008;3(10):e3420. [PubMed: 18923704]
3. Li M, Marin-Muller C, Bharadwaj U, Chow KH, Yao Q, Chen C. MicroRNAs: control and loss of control in human physiology and disease (Review). World Journal of Surgery 2009;33(4):667–84. [PubMed: 19030926]
4. Pan ZW, Lu YJ, Yang BF. MicroRNAs: a novel class of potential therapeutic targets for cardiovascular diseases (Review). Zhongguo Yao Li Xue Bao/Acta Pharmacologica Sinica 2010;31(1):9-1.
5. Nakasa T, Miyaki S, Okubo A, Hashimoto M, Nishida K, Ochi M, et al. Expression of microRNA-146 in rheumatoid arthritis synovial tissue. Arthritis & Rheumatism 2008;58(5):1284–92. [PubMed: 18438844]
6. Xiao B, Wang Y, Li W, Baker M, Guo J, Corbet K, et al. Plasma microRNA signature as a noninvasive biomarker for acute graft-versus-host disease. Blood 2013;122(19):3365–75. [PubMed: 24041574]
7. Ranganathan P, Heaphy CE, Costinean S, Stauffer N, Na C, Hamadani M, et al. Regulation of acute graft-versus-host disease by microRNA-155. Blood 2012;119(20):4786–97. [PubMed: 22408260]
8. Stickel N, Hanke K, Marschner D, Prinz G, Kohler M, Melchinger W, et al. MicroRNA-146a reduces MHC-II expression via targeting JAK/STAT signaling in dendritic cells after stem cell transplantation. Leukemia 2017;31(12):2732–41. [PubMed: 28484267]
9. Chen S, Smith BA, Iype J, Prestipino A, Pfeifer D, Grundmann S, et al. MicroRNA-155-deficient dendritic cells cause less severe GVHD through reduced migration and defective inflammasome activation. Blood 2015;126(1):103–12. [PubMed: 25972159]
10. Sorror M How I assess comorbidities prior to hematopoietic cell transplantation. Blood 2013;121(15):2854–63. [PubMed: 23355537]
11. Xie LN, Zhou F, Liu XM, Fang Y, Yu Z, Song NX, et al. Serum microRNA155 is increased in patients with acute graft-versus-host disease. Clinical Transplantation 2014;28(3):314–23. [PubMed: 24494749]
12. Knouf EC, Wyman SK, Tewari M. The human TUT1 nucleotidyl transferase as a global regulator of microRNA abundance. PLoS ONE [Electronic Resource] 2013;8(7):e69630.
13. Geiss GK, Bumgarner RE, Birditt B, Dahl T, Dowidar N, Dunaway DL, et al. Direct multiplexed measurement of gene expression with color-coded probe pairs. Nat Biotechnol 2008;26(3):317–25. [PubMed: 18278033]
14. Pritchard CC, Cheng HH, Tewari M. MicroRNA profiling: approaches and considerations. Nature reviews Genetics 2012;13(5):358–69.
15. Derda AA, Thum S, Lorenzen JM, Bavendiek U, Heineke J, Keyser B, et al. Blood-based microRNA signatures differentiate various forms of cardiac hypertrophy. International Journal of Cardiology 2015;196:115–22 (doi: 10.1016/j.ijcard.2015.05.185). [PubMed: 26086795]
16. Liu Y, Cai Q, Bao PP, Su Y, Cai H, Wu J, et al. Tumor tissue microRNA expression in association with triple-negative breast cancer outcomes. Breast Cancer Research & Treatment 2015;152(1): 183–91. [PubMed: 26062749]

17. Schaefer JS, Attumi T, Opekun AR, Abraham B, Hou J, Shelby H, et al. MicroRNA signatures differentiate Crohn's disease from ulcerative colitis. BMC Immunology 2015;16:5. [PubMed: 25886994]
18. Sayed AS, Xia K, Li F, Deng X, Salma U, Li T, et al. The diagnostic value of circulating microRNAs for middle-aged (40–60-year-old) coronary artery disease patients. Clinics (Sao Paulo, Brazil) 2015;70(4):257–63.
19. Zhu H, Leung SW. Identification of microRNA biomarkers in type 2 diabetes: a meta-analysis of controlled profiling studies. Diabetologia 2015;58(5):900–11. [PubMed: 25677225]
20. Steen SO, Iversen LV, Carlsen AL, Burton M, Nielsen CT, Jacobsen S, et al. The circulating cell-free microRNA profile in systemic sclerosis is distinct from both healthy controls and systemic lupus erythematosus. Journal of Rheumatology 2015;42(2):214–21. [PubMed: 25399392]
21. Vinuesa CG, Rigby RJ, Yu D. Logic and extent of miRNA-mediated control of autoimmune gene expression (Review). International Reviews of Immunology 2009;28(4-3):112–38. [PubMed: 19811318]
22. Villa C, Fenoglio C, De Riz M, Clerici F, Marcone A, Benussi L, et al. Role of hnRNP-A1 and miR-590–3p in neuronal death: genetics and expression analysis in patients with Alzheimer disease and frontotemporal lobar degeneration. Rejuvenation Research 2011;14(3):275–81. [PubMed: 21548758]
23. Ortega FJ, Mercader JM, Catalan V, Moreno-Navarrete JM, Pueyo N, Sabater M, et al. Targeting the circulating microRNA signature of obesity. Clinical Chemistry 2013;59(5):781–92. [PubMed: 23396142]
24. Gidlof O, Smith JG, Miyazu K, Gilje P, Spencer A, Blomquist S, et al. Circulating cardio-enriched microRNAs are associated with long-term prognosis following myocardial infarction. BMC Cardiovascular Disorders 2013;13:12. [PubMed: 23448306]
25. Adyshev DM, Moldobaeva N, Mapes B, Elangovan V, Garcia JG. MicroRNA regulation of nonmuscle myosin light chain kinase expression in human lung endothelium. American Journal of Respiratory Cell & Molecular Biology 2013;49(1):58–66. [PubMed: 23492194]
26. Gandhi R, Healy B, Gholipour T, Egorova S, Musallam A, Hussain MS, et al. Circulating microRNAs as biomarkers for disease staging in multiple sclerosis. Annals of Neurology 2013;73(6):729–40. [PubMed: 23494648]
27. Ellis KL, Cameron VA, Troughton RW, Frampton CM, Ellmers LJ, Richards AM. Circulating microRNAs as candidate markers to distinguish heart failure in breathless patients. European Journal of Heart Failure 2013;15(10):1138–47. [PubMed: 23696613]
28. Vuppalanchi R, Liang T, Goswami CP, Nalamasu R, Li L, Jones D, et al. Relationship between differential hepatic microRNA expression and decreased hepatic cytochrome P450 3A activity in cirrhosis. PLoS ONE [Electronic Resource] 2013;8(9):e74471.
29. Lin J, Welker NC, Zhao Z, Li Y, Zhang J, Reuss SA, et al. Novel specific microRNA biomarkers in idiopathic inflammatory bowel disease unrelated to disease activity. Modern Pathology 2014;27(4):602–8. [PubMed: 24051693]
30. Ren J, Zhang J, Xu N, Han G, Geng Q, Song J, et al. Signature of circulating microRNAs as potential biomarkers in vulnerable coronary artery disease. PLoS ONE [Electronic Resource] 2013;8(12):e80738.
31. Lu Y, Hou S, Huang D, Luo X, Zhang J, Chen J, et al. Expression profile analysis of circulating microRNAs and their effects on ion channels in Chinese atrial fibrillation patients. International journal of clinical and experimental medicine 2015;8(1):845–53. [PubMed: 25785065]
32. Huang C, Zheng JM, Cheng Q, Yu KK, Ling QX, Chen MQ, et al. Serum microRNA-29 levels correlate with disease progression in patients with chronic hepatitis B virus infection. Journal of Digestive Diseases 2014;15(11):614–21. [PubMed: 25138057]
33. Niu G, Li B, Sun J, Sun L. miR-454 is down-regulated in osteosarcomas and suppresses cell proliferation and invasion by directly targeting c-Met. Cell Proliferation 2015;48(3):348–55. [PubMed: 25880599]
34. Ward JA, Esa N, Pidikiti R, Freedman JE, Keaney JF, Tanriverdi K, et al. Circulating cell and plasma microRNA profiles differ between non-ST-segment and ST-segment-elevation myocardial infarction. Family Medicine & Medical Science Research 2013;2(2):108. [PubMed: 24432306]

35. Mitchell PS, Parkin RK, Kroh EM, Fritz BR, Wyman SK, Pogosova-Agadjanyan EL, et al. Circulating microRNAs as stable blood-based markers for cancer detection. Proceedings of the National Academy of Sciences 2008;105(30):10513–8.

36. Hunter MP, Ismail N, Zhang X, Aguda BD, Lee EJ, Yu L, et al. Detection of microRNA expression in human peripheral blood microvesicles. [Erratum appears in PLoS One. 2010;5(3) doi: 10.1371/annotation/b15ca816–7b62–4474-a568–6b60b8959742] PLoS ONE [Electronic Resource] 2008;3(11):e3694.

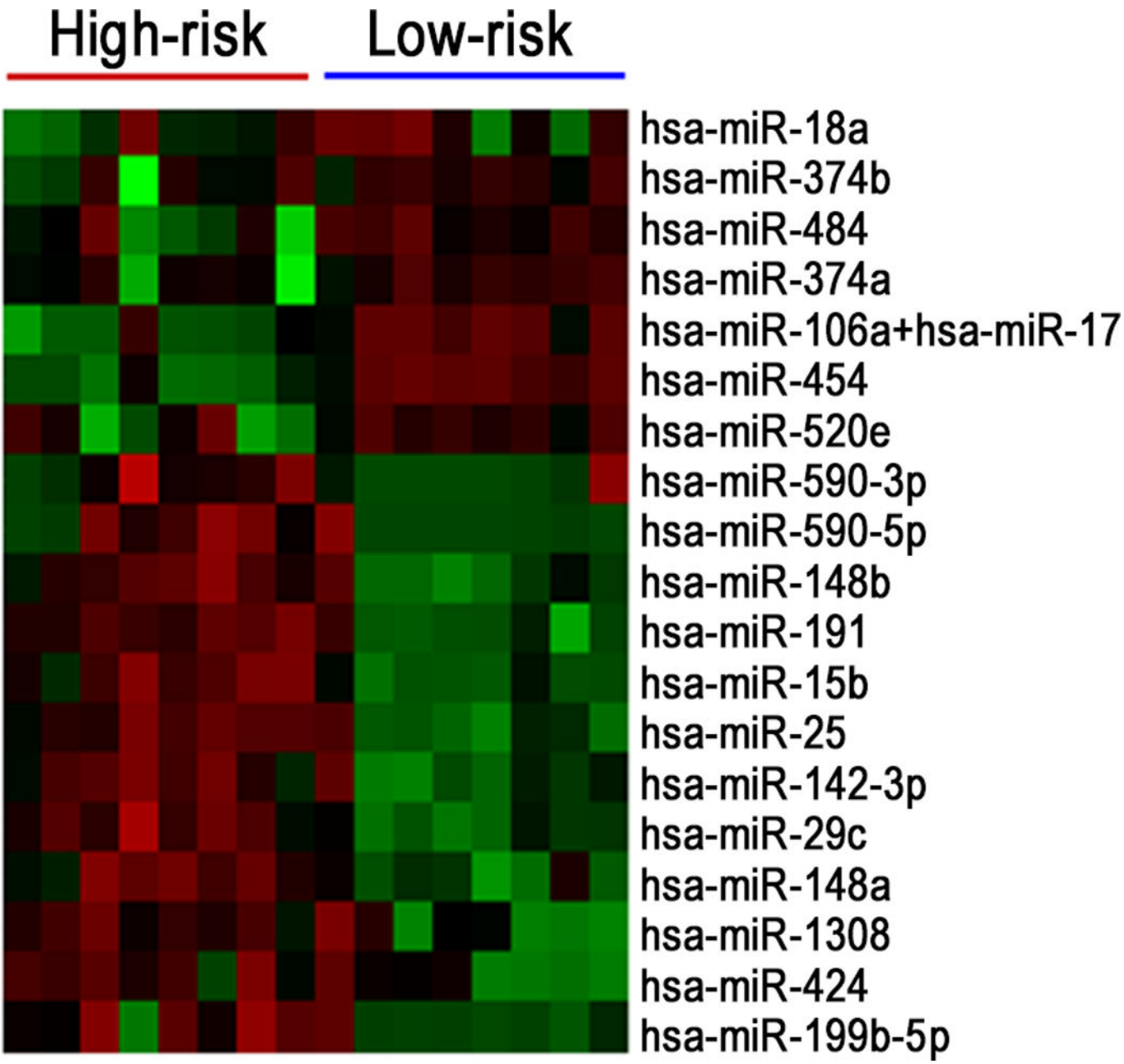

Figure 1.

Agglomerative cluster “heat-map” analysis of 8 samples from high-risk and 8 samples from low-risk groups. The analysis shows differential under-expression of 7 and differential over-expression of 12 miRs between the two groups.

Table 1.

Patient Characteristics

	Low Risk	High Risk
Age		
Mean (years)	48	50
Range (years)	22–70	24–68
< 60 years	72.2%	77.8%
> 60 years	27.8%	22.2%
Gender		
Male	50.0%	50.0%
Female	50.0%	50.0%
Race		
White	88.9%	83.3%
Multiple	0.0%	5.6%
Unknown	11.1%	0.0%
Asian	0.0%	11.1%
Black	0.0%	0.0%
Ethnicity		
Not Hispanic or Latino	100.0%	83.3%
Hispanic or Latino	0.0%	11.1%
Unknown	0.0%	5.6%
HCT-CI		
Mean HCT-CI	0	5.5
HCT-CI Range	0	4–9
0	100.0%	-
4	-	44.4%
5 to 6	-	27.8%
7+	-	27.8%
Disease		
AML	77.8%	66.7%
ALL	22.2%	33.3%
Conditioning regimen		
RIC/NMA	50.0%	61.1%
High	50.0%	38.9%
Disease risk index		
Low	0.0%	0.0%
Intermediate	94.4%	72.2%
High	5.6%	27.8%
Very High	0.0%	0.0%

Table 2.

Fold change of miR expressions comparing high versus low risk groups

miR-	Fold change	P-value
18a	−2.01	0.071
374b	−2.38	0.039
484	−1.59	0.085
374a	−1.62	0.058
106a + 17	−2	0.099
454	−2.38	0.039
520e	−2.72	0.064
590–3p	2.49	0.008
590–5p	4.69	0.047
148b	1.33	0.082
191	1.57	0.011
15b	1.5	0.019
25	1.36	0.08
142–3p	1.81	0.05
29c	1.48	0.039
148a	1.47	0.051
1308	3.19	0.014
424	3	0.031
199b–5p	2.3	0.036

Table 3.

Multivariate analyses, area under the curve (AUC) and odds ratio evaluations of miR expressions between high- and low-risk groups.

miR-	Difference	95% CI	P-value	Effect Size	AUC	Odds Ratio
142–3p	−40,199	−77,907 to −2491	.05	2.09	0.74 (0.58–0.91)	0.15 (0.03–0.87)
191	−407	−728 to −86	.02	2.49	0.81 (0.66–0.96)	0 *
374b	56	8 to 105	.03	2.27	0.75 (0.59–0.92)	9.12 (1.47–56.68)
424	−31	−59 to −3	.04	2.19	0.76 (0.60–0.92)	0.16 (0.03–0.84)
454	24	2 to 45	.04	2.17	0.74 (0.58–0.91)	Infinite **
590–3p	−5	−9 to −1	.03	2.24	0.75 (0.59–0.92)	0.14 (0.02–0.79)
15b	−1266	−2492 to −40	.05	2.02	0.74 (0.58–0.91)	0.29 (0.07–1.30)
29c	−672	−1242 to −102	.03	2.31	0.76 (0.60–0.92)	0.19 (0.04–0.93)

Adjusted mean difference in miR expression between high- and low-risk groups (with 95% confidence interval, p-value), effect size of difference (number of standard-deviation units adjusted difference is away from zero), AUC for expression (95% CI), and odds ratio (95% CI) for low risk between high and low expression.

* Eight of 8 low-expression patients were in low-risk category compared to 10 of 28 high-expression patients

** Seven of 7 high-expression patients were in low-risk category compared to 11 of 29 low-expression patients